



Widespread fracture movements during a volcano-tectonic unrest: the Reykjanes Peninsula, Iceland, from 2019–2021 TerraSAR-X interferometry

Cécile Ducrocq¹ · Thóra Árnadóttir¹ · Páll Einarsson¹ · Sigurjón Jónsson² · Vincent Drouin³ · Halldór Geirsson¹ · Ásta Rut Hjartardóttir¹

Received: 24 July 2023 / Accepted: 12 December 2023 / Published online: 13 January 2024

© The Author(s) 2024

Abstract

Tectonic controls on dyke emplacements, eruption dynamics and locations have been observed in multiple volcanic areas worldwide. Mapping of active structures is therefore key for assessing potential tectonic and volcanic hazards in active regions. We used wrapped interferograms from the TerraSAR-X satellite to map active fracture movements over a 2-year period of a volcano-tectonic unrest at the onshore Reykjanes Peninsula plate boundary in SW Iceland. As of 1 December 2023, the unrest has included at least six inflation events and five dyke injections resulting in three eruptions of the Fagradalsfjall volcanic segment. In addition to the deformation associated with the 2019–2021 inflation events and intrusions, the interferograms reveal fracture movements over a wide area surrounding the active plate boundary segment. This first-order mapping of active fractures complements previously mapped structures, as InSAR allows for the detection of subtle ground movements, even in areas where young lava flows cover older structures. Our fracture data therefore fill in some of the apparent voids in previous fracture and fault maps of SW Iceland. Furthermore, our investigation reveals aseismic movement on previously unknown fractures directly beneath the town of Grindavík, as well as a N45° E striking fracture co-located with the longest lasting volcanic vent of the subsequent 2021 eruption. The mapping method we present in this study is relevant for active volcano-tectonic regions where InSAR can be applied to detect small-scale fracture movements to advance understanding of ongoing unrest and volcano-tectonic hazards.

Keywords Volcano-tectonic unrest · Reykjanes Peninsula oblique rift · Fracture mapping · InSAR · Aseismic movement · Volcano-tectonic hazards

Introduction

Interactions between tectonics and volcanic features have been widely documented in rift zones around the world, e.g.

Editorial responsibility: A. Tibaldi

✉ Cécile Ducrocq
cad7@hi.is

Halldór Geirsson
hgeirs@hi.is

¹ Nordic Volcanological Center, Institute of Earth Sciences, University of Iceland, Sturlugata 7, Askja, Reykjavík IS-102, Iceland

² King Abdullah University of Science and Technology, Thuwal, Saudi Arabia

³ Icelandic Meteorological Office, Bústaðavegi 9, Reykjavík IS-105, Iceland

in Afar, Krafla, Taupō Volcanic Zone and Holuhraun (Dobre and Peltzer 2007; Dumont et al. 2016; Einarsson 2008; Einarsson and Brandsdóttir 2021; Hjartardóttir et al. 2012, 2016; Ruch et al. 2016; Seebeck and Nicol 2009; Villamor et al. 2011, 2022). Surface fracturing and fracture movements result from stress and strain changes in the shallow crust, induced by subsurface processes, such as faulting and volumetric changes. Pre-existing fractures, regional tectonics and related processes can influence magmatic pathways and dynamics, for example, location of eruptive activity, dyke propagation and emplacement (e.g. Monaco et al. 2005; Kühn and Dahm 2008; Spacapan et al. 2016; Hjartardóttir et al. 2023). Therefore studies of active tectonics prior to and during a volcano-tectonic unrest can yield useful information for future monitoring and hazard assessment of the region affected. However, detailed regional-scale observations of fracture formation and reactivation during such an

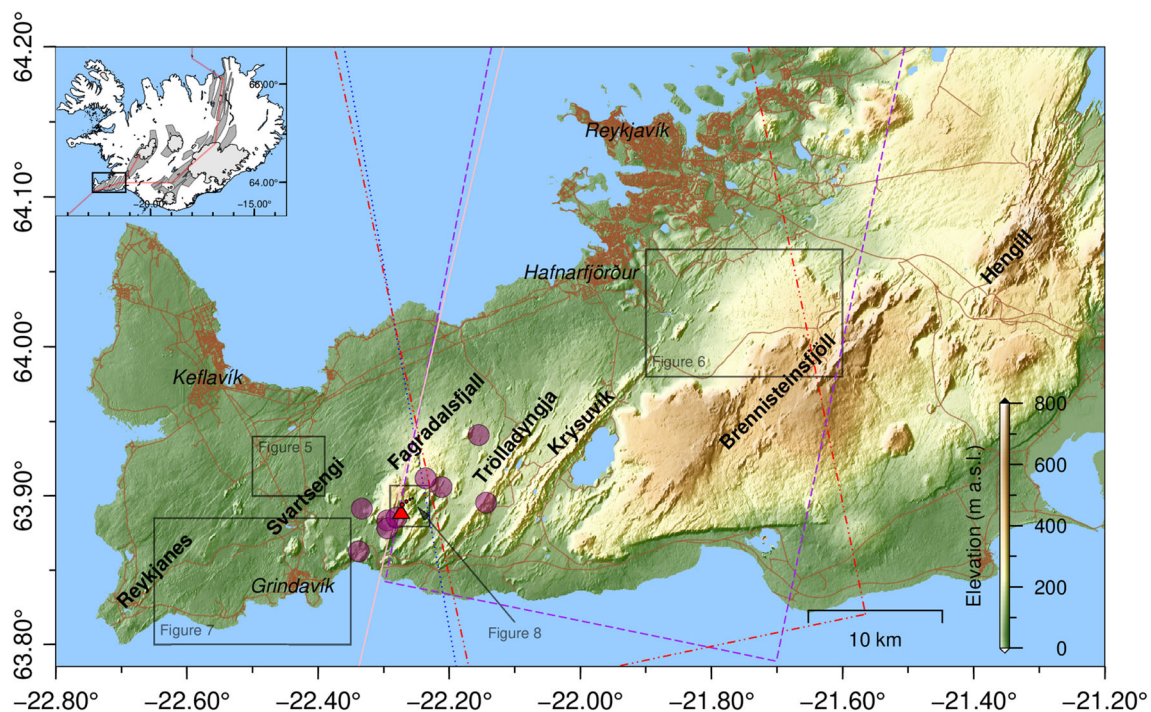


Fig. 1 Elevation map of the Reykjanes Peninsula (RP) from the ArcticDEM (v1.0.0; Porter et al. 2018, modified by National Land Survey of Iceland). Names of the main volcanic areas are written in bold, while major settlements are in italics. Epicenters of M 5–5.6 earthquakes in 2019–2021 are shown as purple circles. The red triangle indicates the location of the 2021 Fagradalsfjall eruption. The extent of TerraSAR-X

images from ascending tracks 26 (blue dots) and 117 (red dots and dashes) and descending tracks 34 (purple dashes) and 110 (pink line) is indicated. The inset shows the location of the RP in south-west Iceland, with the red lines showing the main plate boundary axes (Árnadóttir et al. 2009)

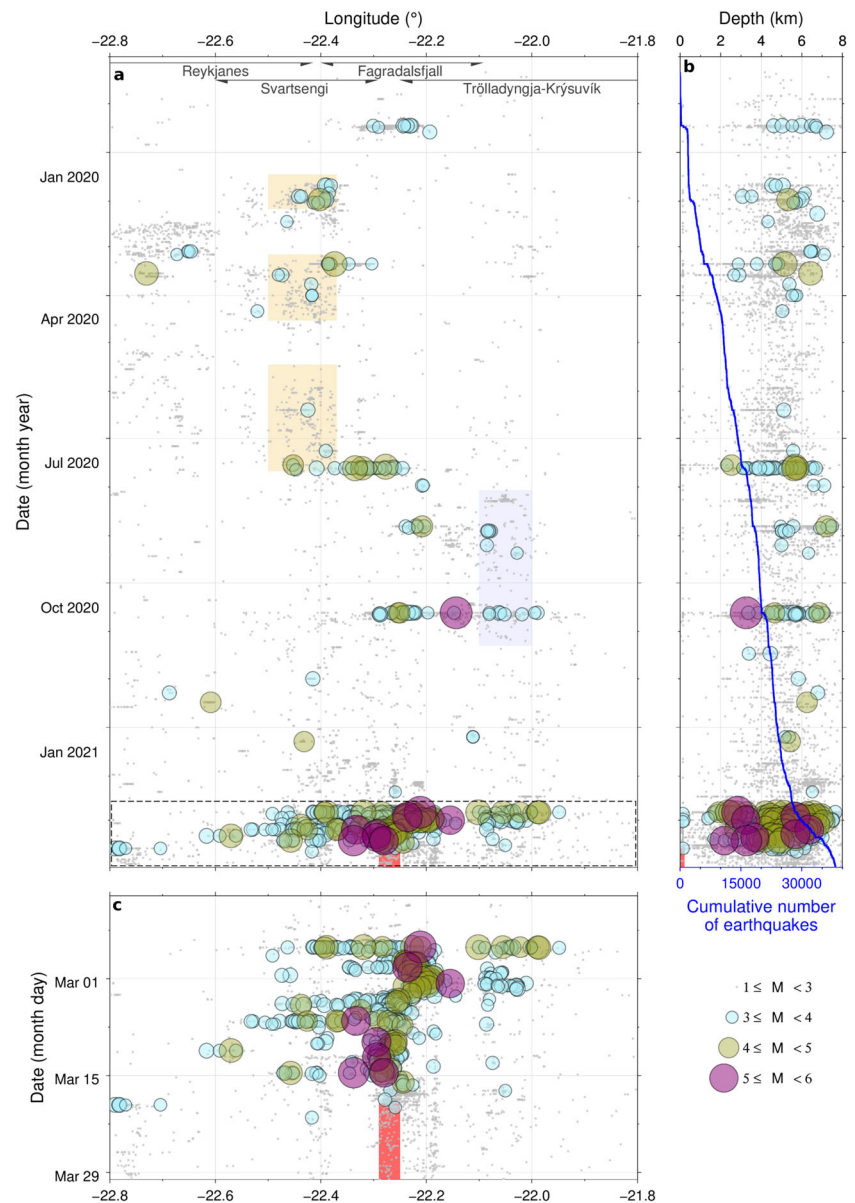
unrest period preceding an eruption are difficult, and few have been documented.

The Mid-Atlantic ridge comes onshore at the SW tip of Iceland in a ~ 70 km long segment of trans-tensional rifting on the Reykjanes Peninsula (RP; Fig. 1). Six separate volcanic areas can be distinguished across the RP, from west to east: Reykjanes, Svartsengi, Fagradalsfjall, Trölladyngja-Krýsuvík (later referred to as Krýsuvík), Brennisteinsfjöll and Hengill (see Fig. 1; Sæmundsson et al. 2020). These volcano-tectonic areas feature normal faults, open fractures, eruptive fissures, and prominent hyaloclastite ridges formed in subglacial fissure eruptions, trending $N30\text{--}40^\circ$ E (Einarsson 2008). The strain of the plate boundary is accommodated through a combination of strike slip on faults striking $\sim N0 \pm 10^\circ$ E (i.e. bookshelf faulting; Einarsson 2008) and normal motion on faults striking $\sim N30\text{--}60^\circ$ E. Strike-slip faults are confined within an E-W trending 3–5 km wide zone centred on the plate boundary axis, while normal-fault structures extend to the NE and SW of this zone (Clifton and Schlische 2003; Clifton and Kattenhorn 2006). The youngest pre-2021 lavas on the peninsula cover older fault structures and have so far prevented their mapping (Clifton and Kattenhorn 2006).

Historically, eruptive activity has occurred at different parts of the RP with extended periods of relative quiescence

(800–1000 years; Sæmundsson et al. 2020). The last eruptive episode on the RP, prior to the 2021 eruption in Fagradalsfjall, was 750–1100 years ago (Sæmundsson et al. 2020). The development of geodetic methods since the 1990s has helped to document multiple non-eruptive volcanic unrest episodes across the peninsula: e.g. Krýsuvík ($\sim 2007\text{--}2009$, 2010–2011; Michalczevska et al. 2012; Gudjónsdóttir et al. 2020) and Hengill (1993–1999, 2017–2018; Feigl et al. 2000; Hreinsdóttir et al. 2001; Ducrocq et al. 2021). Intense earthquake sequences with events of magnitude M 5–6.1 were recorded, in different parts of the peninsula, in 1928–29, 1952, 1955, 1967–70, 1973, 1993–1999, 2000, 2003, 2011, and 2013 (Pagli et al. 2003; Árnadóttir et al. 2004; Keiding et al. 2008, 2009; Sudhaus and Jónsson 2009; Björnsson et al. 2020; Einarsson et al. 2020; Jónsson et al. 2021, and references therein). Interferometric synthetic aperture radar (InSAR) studies have noted aseismic fault movements and deformation associated with low-to-moderate magnitude earthquakes ($M \leq 4$) across the RP (Feigl et al. 2000; Jónsson 2009; Keiding et al. 2010; Michalczevska et al. 2012). Comparison of geodetic and seismic moment in the Reykjanes and Krýsuvík volcanic areas shows that the seismic moment is generally smaller, indicating partial aseismic moment release (e.g. Árnadóttir et al. 2004; Keiding et al. 2010).

Fig. 2 Timing versus (a, c) longitude and (b) depth of earthquakes ($1 \leq M < 5.6$) recorded above 8 km depth from 1 November 2019 to 30 March 2021 between Reykjanes (west) and Krýsuvík (east) volcanic areas. The yellow, blue and red areas indicate the approximate duration and locations of the unrests in the Svartsengi and Krýsuvík areas, and the 2021 eruption in Fagradalsfjall, respectively (Cubuk-Sabuncu et al. 2021; Flóvenz et al. 2022). The cumulative number of earthquakes is shown as a blue line in (b). (c) Close-up of the earthquakes from 17 February to 30 March 2021 (dashed box in panel a). M refers to local magnitudes from the catalogue of Icelandic Meteorological Office (Panzer et al. 2016)



Sustained seismicity above background levels on the RP started in December 2019 near Fagradalsfjall (Fig. 2). Three consecutive periods of uplift were detected via geodetic and seismic data in the Svartsengi volcanic area between January and July 2020 (Cubuk-Sabuncu et al. 2021; Flóvenz et al. 2022; Geirsson et al. 2021). Concomitantly, an inflation was noted in the Reykjanes volcanic system in February 2020 (Geirsson et al. 2021). In July 2020, the seismicity appears to have then migrated eastward from Svartsengi to Fagradalsfjall, followed by a 5 mm/month uplift in the Krýsuvík volcanic area between August and November 2020 (Fig. 2; Flóvenz et al. 2022). The seismicity associated with the 2020 Krýsuvík uplift was mostly below M 4 until the 20 October 2020 M 5.6 earthquake and its aftershock sequence (Fig. 2).

In late February 2021, widespread ground deformation and increased seismicity (eight M 5–5.6 events) indicated that magma was migrating to shallow depths in the Fagradalsfjall area, leading to an eruption that started on 19 March 2021 (Figs. 1 and 2; Sigmundsson et al. 2022; Barsotti et al. 2023). Between the 5 and 14 of April, new fissures opened north of the first vents, with effusive eruption observed simultaneously in several vents (Barsotti et al. 2023). Effusive activity was focused on a single vent from 27 April until the end of the eruption on 18 September 2021 (Barsotti et al. 2023; Pedersen et al. 2022; Eibl et al. 2023; Lamb et al. 2022). Interestingly, focused deformation along a section of the plate boundary was detected during the dyke intrusion (Sigmundsson et al. 2022), similar to what was observed between

Svartsengi and Krýsuvík during July–October 2020 (Figure S26). Sigmundsson et al. (2022) relate this deformation to increased left-lateral shearing along the plate boundary and note that increased shear strain was measured in Fagradalsfjall between 2015 and 2018. Subsequent short-lived effusive eruptions occurred on the Fagradalsfjall volcanic area during 3–21 August 2022 and 10 July–5 August 2023 (Figure S8; Venzke 2023). On 27 October 2023, renewed inflation was detected using GNSS and InSAR in Svarstengi, and on 10 November 2023, a dyke intrusion propagated beneath the town of Grindavík. As of 1 December 2023, unrest on the Reykjanes Peninsula is ongoing (<https://en.vedur.is/>).

In this study, we take advantage the high spatial and temporal resolution of InSAR to map active surface fracture movements on the RP, spanning from 22.8° W to 21.6° W, during the volcano-tectonic sequence that began in December 2019 until the onset of the first eruption in March 2021. These fracture movements indicate reactivation of possibly pre-existing fractures, many of which have not been mapped before.

Data and methods

Synthetic Aperture Radar (SAR) images from the TerraSAR-X satellite (TSX) of the German Aerospace Center were ordered via the Icelandic Supersite project to monitor the unrest on the RP between December 2019 and March 2021. Particularly, four TSX tracks, two descending: 110 and 34, and two ascending: 26 and 117 (Table 1), cover the ~50 km segment of plate boundary where most of the seismicity and deformation were located (Figs. 1 and 2). The StripMap SAR images, 50 km × 30 km footprint in azimuth and range, from the TSX satellite, have ~3 m ground resolution along and across-track. The high ground resolution and short X-band radar wavelength (~3.1 cm), make these data ideal to study subtle fracture movements (e.g. Richter et al. 2013).

We used the DORIS software (Kampes et al. 2003) to produce high resolution interferograms between small temporal-baseline images (return time of the satellite: 11

days). We set the multilooking parameter to 4, to reduce speckle noise, yielding a pixel size of ~12 m along and across-track. Additional interferograms were created to cover events of significant deformation (e.g. M 4.5–5.6 earthquakes), as well as interferograms with longer temporal baselines to detect subtle cumulative motion or to minimize the perpendicular baseline (B_{perp}) between a pair of images. The topographic phases were estimated using the ArcticDEM (Porter et al. 2018, modified by National Land Survey of Iceland), resampled to 10 m, and removed from the generated interferograms. To assist the precise mapping of the fault and fractures locations, we filtered the interferograms using the Goldstein filter ($\alpha=0.8$; Goldstein and Werner 1998) on overlapping blocks (blocksize=32 and overlap=15) in order to generate interferograms with less decorrelation noise while retaining sharp discontinuities. We used the wrapped interferograms in radar coordinates to manually identify and map linear phase discontinuities using QGIS (Fig. 3; QGIS Development Team 2021), which we later converted into WGS84 coordinates.

As it can be difficult to distinguish between combinations of atmospheric noise, topographic errors, and real discontinuities, we assigned a quality index (QI) to each mapped discontinuity based on visual assessment of the mapping confidence: numbers 1, 2, or 3, corresponding to certain, likely, and probable. We also estimated the dominant sense of motion and amplitude of each mapped discontinuity (Supplemental Material Section S6). Sense of motion and amplitude are strictly indicative, as wrapped interferograms only exhibit one-dimension line-of-sight (LOS) projections of the true three-dimensional deformation field.

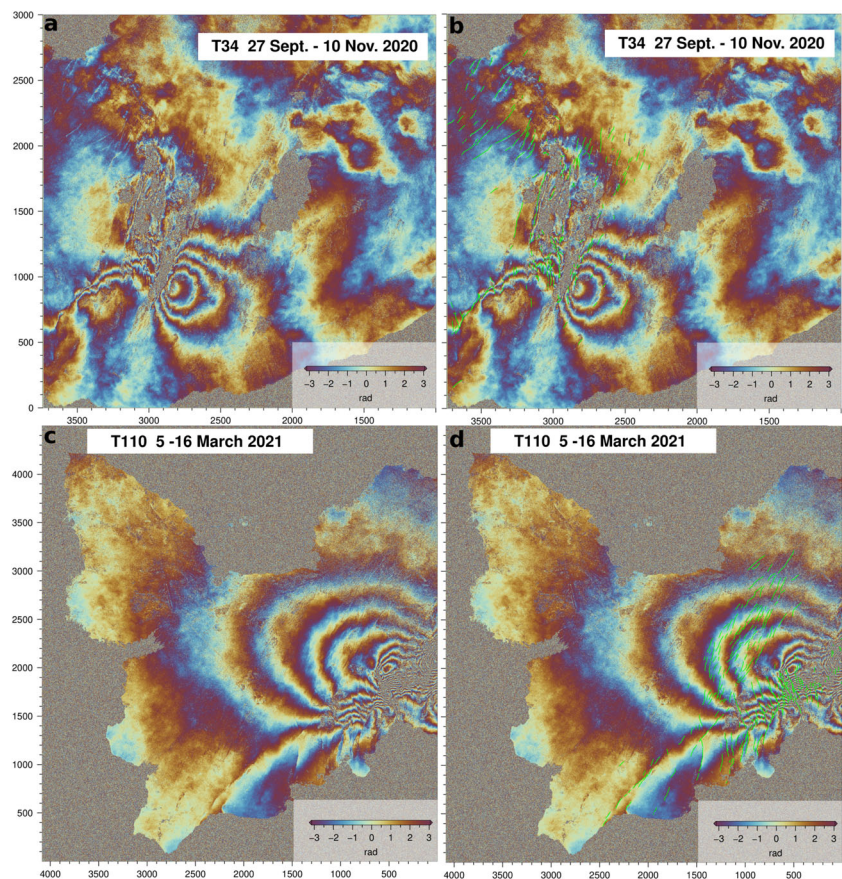
Results

We manually mapped ~2500 discontinuities in 54 interferograms (Fig. 4; Tables 1 and S1). As two tracks, ascending and descending (Fig. 1), cover approximately the same area on the ground, we find that around 1250 independent discontinuities have been identified during the December 2019–March 2021 unrest period on the RP. About 35 % of the mapped discontinuities have a QI of 1 or 2, i.e. ~450 of the 1250 discontinuities. Of those, 70% have inferred LOS movement above 5 mm, resulting in clear discontinuities in the wrapped interferogram, reflected by our high confidence of the discontinuity mapping (Supplementary Sections S2 and S6 discuss the limitation of our mapping method). Structures with QI=3, small LOS amplitude (<7 mm) or length <500 m may not be observable via the different track geometries and hence less reliable, but are included here for completeness (Supplementary Section S2). The mapped discontinuities mainly strike N10° E to N40° E, however, populations of N10° W and N50° E are also observed (Fig. 4). Mapped lin-

Table 1 Mean heading and incidence angles, and number of individual interferograms used for mapping for each of the TerraSAR-X tracks (26, 34, 110 and 117)

Track number	Mean heading (° N)	Mean incidence (°)	Number of interferograms used for mapping
26	349.4	43.3	23
34	191.7	39.3	13
110	193.1	32.9	12
117	347.8	37.0	6

Fig. 3 Wrapped interferograms in radar geometry from descending tracks 34 and 110 spanning 27 September to 10 November 2020 (panels a and b; $B_{\text{perp}} = 10.1$ m) and, 5–16 March 2021 (panels c and d; $B_{\text{perp}} = 25.5$ m), respectively. The green lines in (b) and (d) show discontinuities mapped in this study



ear phase discontinuities are interpreted as surface fracture movements, some of which can be summarized as delineating larger subsurface structures which include, not exclusively, faults.

Most of the fracture movements we map are located close to, or within areas of intense deformation and seismicity during the time of our study (December 2019–March 2021; Figs. 1, 2, 4 and S13–S17). Relatively few fractures were mapped east of longitude 22° W (Figs. 4 and S13) during this time. Our study indicates that fractures in the areas SW and NE of the inflation centres in the Svartsengi volcanic area moved during January–July 2020, at the start of the episode covered by our study (Figs. 4, 7 and S14). Detailed analysis suggests that only a small number of fractures were activated during this time (see Supplement Section S8). During the summer of 2020, we identify at least five fractures, partly associated with \sim M 4–5 earthquakes in the Fagradalsfjall volcanic area (Figs. 2, 4, S14 and S15). In data from October 2020, most of the discontinuities we mapped are located in the epicentral area of the M 5.6 earthquake of 20 October 2020 (Figs. 2, 4 and S16). In data from February 2021, we mapped fracture movements in the volcanic regions surrounding and including Fagradalsfjall most likely stemming from the dyke intrusion, subsurface faulting, and movement along the plate boundary (Figs. 2, 4 and S17).

In summary, we have detected sub-millimetre movement of fractures across a large area of ~ 900 km², extending from the Reykjanes volcanic area in the west to the Krýsuvík volcanic area in the east (Fig. 4). The number of actively moving fractures decreased sharply after the onset of the March 2021 eruption, concomitant of declining seismicity rates (Fig. 2). An additional long-term syn-eruptive interferogram shows fracture movement ~ 2 km NE of Grindavík, between 17 June and 24 September 2021 (Figure S19), on a structure mapped in our study (Fig. 7a), establishing that the mapped structures presented in our study can be reactivated in future episodes of unrest. Finally, this study presents the potential of InSAR monitoring to detect a first-order of active fracture movements, identifying areas requiring further surveying and ground mapping, which can support volcano-tectonic hazard assessment and informing the nearby communities.

Discussion

We mapped around 1250 independent structures activated during the 2019–2021 volcano-tectonic sequence on the RP using wrapped interferograms. Below, we elaborate on the fractures mapped in this study, describe interactions between the magmatic activity and the complex tectonics of the area,

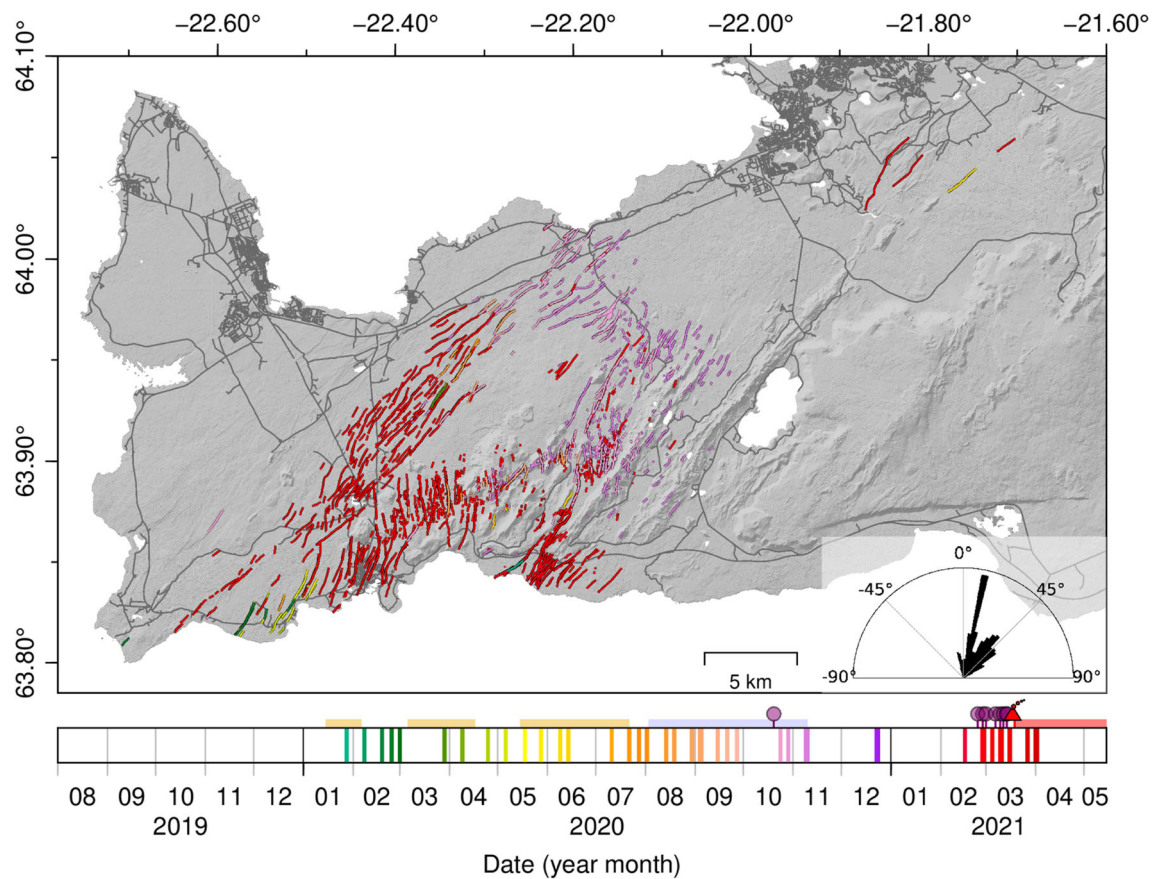


Fig. 4 Fractures mapped from our analysis colour-coded by the estimated date of activation. The vertical bars in the timeline correspond to the acquisition date of the second image of the interferometric pair used to map the fractures. The M 5–5.6 earthquakes (coloured dots), periods of inflation (yellow and blue horizontal bars), onset (red triangle) and

period of eruptive activity (red horizontal bar) from Fig. 2 are shown above the time line. The inset rose diagram shows the overall distribution of the ~ 1250 fracture orientations (between -90° and 90° from north)

and discuss implications for volcanic and tectonic hazard assessments on the peninsula.

Comparison to previously mapped fractures

Overall, our study revealed similar sets of structures on the peninsula as previously described by Clifton and Kattenhorn (2006); Einarsson et al. (2020, 2023); Bufféral et al. (2023) and Hjartardóttir et al. (2023), for example, N-S, $N30^\circ\text{--}45^\circ\text{ E}$, and $N45\text{--}60^\circ\text{ E}$ striking structures (Fig. 4). Our analysis shows that approximately 85% of the fractures we identified were not included in the dataset compiled by Clifton and Kattenhorn (2006, Figure S9). The major increase in mapped fractures can be justified by the different methodologies used. Clifton and Kattenhorn (2006) relied on optical images and ground-based field mapping and only mapped clear tectonic structures, usually with significant vertical offset on the order of decimetres to metres. Using X-band InSAR, we detected fracture movements with LOS amplitude

down to 1–3 mm, often on very minor structures without clear offsets on the ground (e.g. Fig. 5). Furthermore, pre-existing structures covered by young lava flows (younger than 1100 years old), north and south-southwest of the Svartsengi and between the Fagradalsfjall and Krýsuvík volcanic areas were previously undetected (Figs. 4, 5, 7 and S18, locations shown in Fig. 1). Infrastructure and vegetation growth may have impeded mapping of fractures in areas such as Grindavík from recent optical images (Figure S27).

Tectonic implications

We report fracture movements on several structures directly beneath the town of Grindavík (Fig. 7b). Although we cannot correlate specific seismic events to individual active fractures, we observe LOS offset up to 15 mm on these structures (Figure S18). No moderate size earthquake was located on these fractures during the time spanned by the InSAR images (5–16 March 2021). Therefore, these fractures were most likely pre-existing (Fig. S9c and S27) and the offsets we

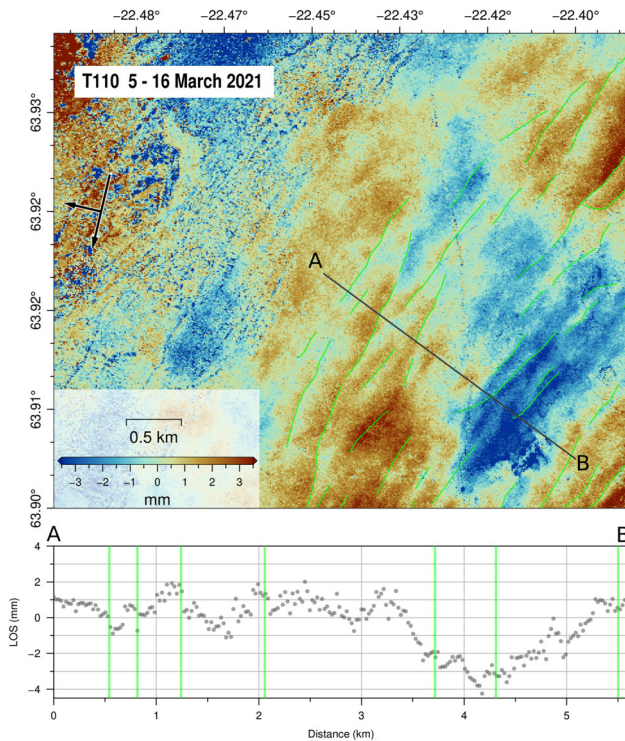


Fig. 5 Example of the reactivation of multiple surface fractures (green lines on map and profile) ~8 km NW of Grindavík (location in Fig. 1). The geocoded unwrapped interferogram (using SNAPHU; Chen and Zebker 2001) from track 110 spans 5–16 March 2021 and has been corrected for large-scale deformation gradient using a quadratic trend. Negative values indicate ground motion away from the satellite, and positive toward the satellite, respectively. The profile (A-B) shows the small amount of movement on these structures (less than ±3 mm offsets in the LOS direction of the satellite)

observed could have been triggered by strong ground shaking, or a response to widespread stress changes due to the

complex activity ($M > 4$ earthquakes, dyke intrusion, motion along the plate boundary) in early March 2021, occurring only ~2–3 km NE of Grindavík (Figures S13 and S17; Sigmundsson et al. 2022). Future detailed seismic (e.g. relative relocation, microseismicity) and strain analysis are needed to improve our understanding on the physical triggers of these fracture movements. The ability to map previously unknown active faults running through the town has important implications for planning authorities. Much of our mapping in Grindavík revealed previously undetected structures, and only small fractures were seen in pavement along some of these structures’ traces. On 10 November 2023, a 15 km long dyke intrusion propagated from NNE-SSW beneath the town of Grindavík, causing major damage and the town to be evacuated. Indeed, some of the fractures we mapped in our study period (December 2019–March 2021) appear to have been reactivated during this intrusion, with up to meter-scale offsets observed in the graben formed over the intrusion (<https://en.vedur.is/> and Figure S9c).

Movements on parallel NE striking fractures were identified NE of the Krýsuvík volcanic area in 2019–2020 (Fig. 6a). Subsurface movement on similar parallel structures were also observed in this area during the eruption in April 2021 (Fig. 6b), and earlier in 1998–1999 (Jónsson 2009). Most of these fracture movements appear to be located away from the recent activity and may therefore be similar to faulting previously documented west of the Reykjanes volcanic area (Keiding et al. 2009, 2010). These structures, including others mapped in this study, may be activated as a gradual response of longer-term tensile motion of the tectonic plates.

Árnadóttir et al. (2004) and Keiding et al. (2009, 2010) noted the discrepancy between relatively large fault movements of tectonic events on the RP compared to their

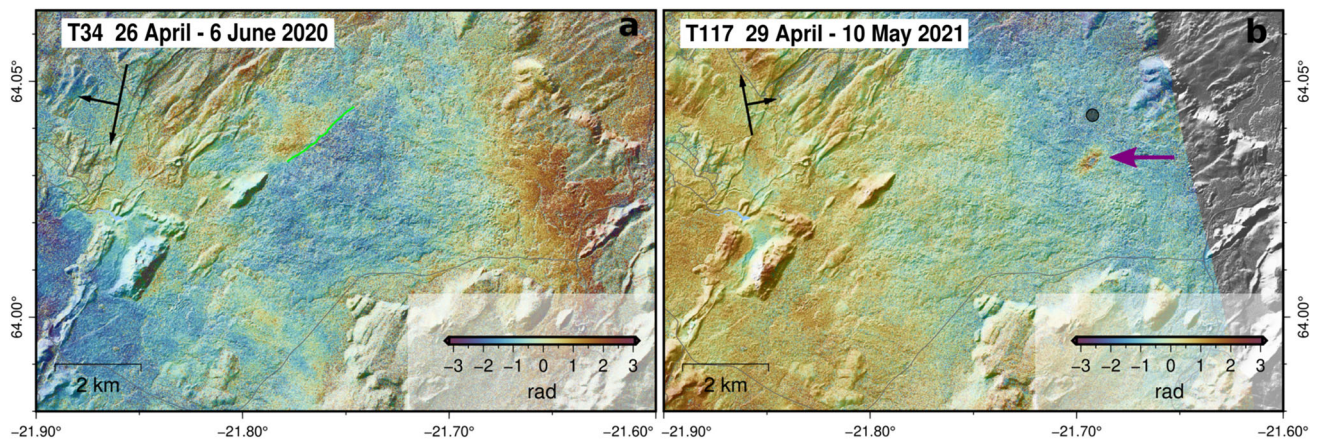
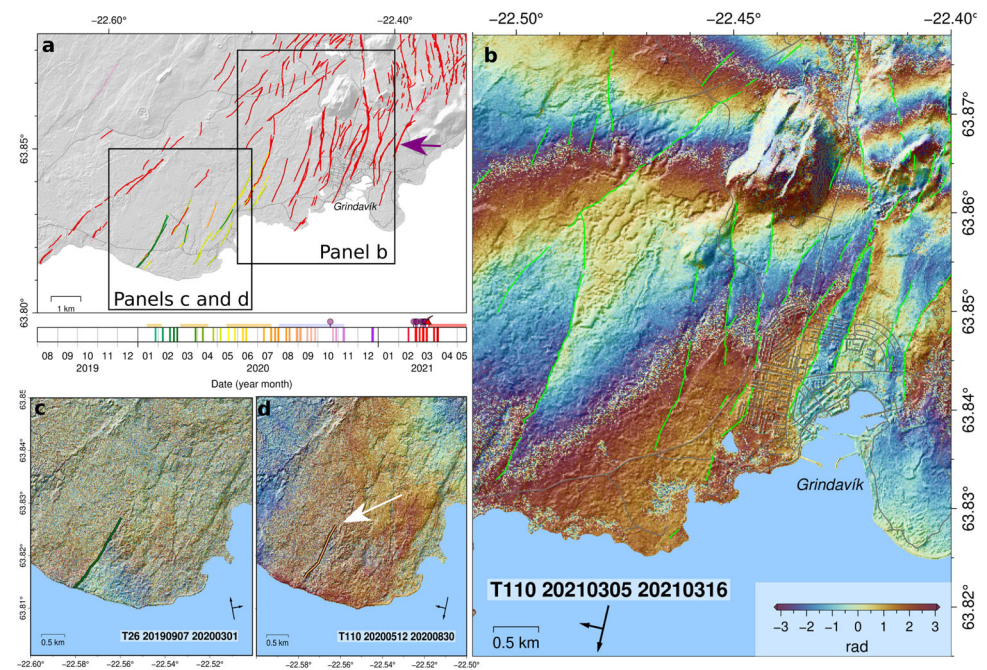


Fig. 6 Wrapped interferograms of the Helgafell area, NE part of the Krýsuvík volcanic area (see location in Fig. 1), from (a) descending track 34 spanning 26 April to 9 June 2020 and (b) ascending track 117 spanning 29 April to 10 May 2021. Panel (a) shows aseismic fracture movement (green line) during the pre-eruptive period, whereas panel

(b) shows small ground deformation (~8 mm; tip of purple arrow) from syn-eruption normal faulting, without rupturing the surface, potentially related to a $M 2.7$ earthquake recorded 8 May 2021 at ~4 km depth (black dot, ~1 km north of the observed ground deformation)

Fig. 7 Examples of the fractures mapped in the vicinity of the town of Grindavík (a), colour-coded by time (same as in Fig. 4). The discontinuity at the tip of the purple arrow (panel a) appears to be active during the eruptive period (Figure S13). (b) Wrapped interferogram from track 110 spanning 5–16 March 2021 shows significant fracture movements (light green lines) through the town of Grindavík and its vicinity associated with intense seismicity (M 5–5.6) and dyke intrusion (see also Figure S12). Wrapped interferograms in panels (c) and (d) highlight a structure activated (green and orange lines, at the tip of the white arrow in the latter panel) during two time spans: 7 September 2019–1 March 2020 (c, ascending track 26) and 12 May–30 August 2020 (d, descending track 110)



relatively small seismic moment. Aseismic movement of fractures has therefore been suggested before on the peninsula. The question of aseismic fracture movement is important, particularly when performing risk assessment for local infrastructure on the peninsula, such as buildings, water pipes or underground cables. In our study, we detected many fracture movements without the corresponding magnitude events in its vicinity, e.g. around Svartsengi during January–July 2020 (Figs. 7 and S14). However, future studies may highlight further detailed evidence for aseismic fracture movements on the RP.

Volcano-tectonic implications

The temporal sequence of active fracture movements we find during 2019–2021 emphasizes the interactions between volcanic and tectonic activity of the RP and the response of the shallow crust to this activity (Figures S14–S17). A key illustration of such interactions are the fractures observed prior to and likely related to the 2021 Fagradalsfjall eruption. Figure 8 highlights the correlation between mapped discontinuities (green lines) from a pre-eruptive interferogram spanning 30 June–15 September 2020 (Fig. 8a), and syn-eruptive deformation spanning 2–13 April 2021 (Fig. 8c) when a new eruptive fissure opened. With movement detected almost continuously between 11 July and 22 October 2020, this N45° E striking fracture was probably activated as a response to the volumetric strain caused by the unrest in the adjacent Svartsengi and Krýsuvík volcanic areas and motion along the plate boundary (Figs. 2, S20 and S27). Locally, this ~2 km long fracture appears to coincide with the even-

tual location of the largest and longest-lived volcanic vent of the 2021 eruption (Fig. 8), and was likely reactivated during the onset of the eruption (Hjartardóttir et al. 2023). Seismic relocations prior to the Fagradalsfjall eruption may delineate an underlying N45° E striking structure beneath the volcanic area (Fischer et al. 2022). It is thus possible that this N45° E surface fracture represented a pre-existing weakness in the crust that influenced the eventual location of the main eruptive vent. Finally, this fracture may be the surface expression of a deeper conjugate system, generating a zone of low compressive stress favouring the ~N30° E orientation of dyke emplacements observed in the area (further discussed by Einarsson et al. 2023; Hrubcová and Vavryčuk 2023).

A significant amount of ground deformation, reaching 10 cm (Flóvenz et al. 2022), and seismic activity between September and July 2020 was also associated with the inflation episodes in the Svartsengi volcanic area (Cubuk-Sabuncu et al. 2021; Flóvenz et al. 2022, Fig. 2). We observed repeated fracture movements up to 9 km SW and NE of the main uplift and subsidence centres (Figs. 4 and 7). These ~N30° E structures are also evident in published Sentinel-1 time series and wrapped interferogram of Cubuk-Sabuncu et al. (2021) and Flóvenz et al. (2022).

Here, we estimate the seismic moment of an event needed to create this offset at the surface (~7 mm). We assume a vertical fault with length of 1.5 km, extending from the surface to 2 km depth, and normal slip of 1 cm. As the fracture is observed at the surface, we use two different shear moduli, 30 GPa, intact rock value used in prior deformation studies in Iceland, and a low one, 2 GPa for the more fractured media (Heap et al. 2020). From these parameters, we esti-

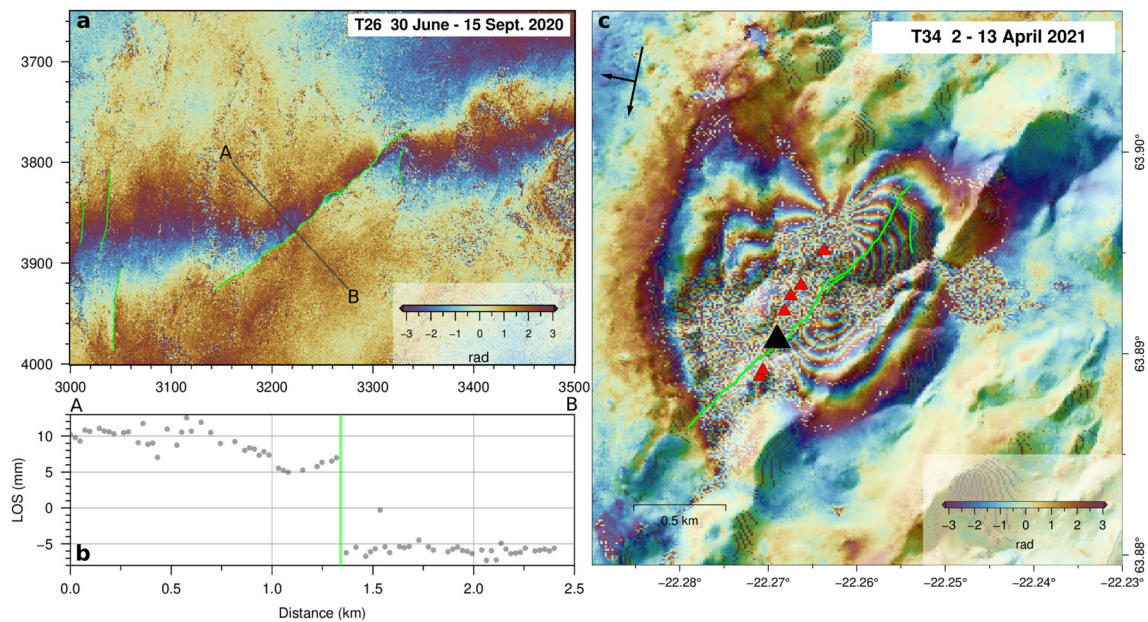


Fig. 8 (a) Wrapped interferogram from ascending track 26 spanning 30 June to 15 September 2020 in radar geometry. (b) Profile A-B (location shown in a) across the unwrapped interferogram (using SNAPHU; Chen and Zebker 2001) and discontinuities (green lines) shown in panel a. Positive values indicates LOS motion towards the satellite (in mm). (c) Filtered wrapped interferogram of descending track 34 spanning 2–13 April 2021; this time period spans the opening of new eruptive fissures

and vents (red triangles; Pedersen et al. 2022). By May, the eruptive activity was concentrated on a single vent, shown by the black triangle. The main incoherent areas show the lava extent across Geldingadalir and a neighbouring valley. The discontinuities (green lines) mapped from the interferogram in panel (a) are overlaid on (c) to highlight the relation between tectonic and volcanic features

mate seismic moment of $M_W 3.9$ or $M_W 2.9$, for the higher and lower shear moduli, respectively (for details see Supplement Section S12). The earthquakes located in this area between 7 September 2019 and 30 August 2020 were all smaller than $M 2$ (Figs. 2 and S14). The Svartsengi inflation sources increased the normal tensile stress on $N30^\circ E$ striking faults located SW and NE of source (Figure S25; source parameters from Flóvenz et al. 2022). We infer that these fracture movements most likely reflect the crustal response of deeper strain change in each intrusive period between 15 January and 22 July 2020.

Conclusions

We mapped around 1250 individual fractures activated during the 2019–2021 volcano-tectonic unrest on the Reykjanes Peninsula (RP), an onshore oblique rifting plate boundary in SW Iceland, using wrapped interferograms. During the study period, several inflation episodes in Svartsengi and Krýsuvík volcanic areas, the 2021 dyke intrusion in Fagradalsfjall and motion along the plate boundary triggered nine moderate size earthquakes and widespread surface fracture movements along ~ 50 km long portion of the RP. Approximately 85% of the fractures mapped in this study were previously undetected, improving our knowledge of tectonic structures in

the region, particularly in the Svartsengi, Fagradalsfjall and Krýsuvík volcanic areas. A few of the identified fractures pass through the town of Grindavík, calling for a reassessment of the tectonic hazard on the RP as the 10 November 2023 intrusion brought to light. We further show a plausible relation between a $N45^\circ E$ fracture activated 6-months prior to the 2021 dyke intrusion, and the largest vent of the 2021 Fagradalsfjall eruption. Lastly, we discuss that potential background tectonic fracture movements occur sporadically and partly aseismically, without intense volcano-tectonic unrest on the RP. Altogether, this study brings new knowledge to better prepare the communities on the RP for ongoing and future volcanic and tectonic events as well as highlighting pre- and syn-eruptive surface processes that may be observed in volcano-tectonic regions around the world.

Supplementary information

Attached to this main text is Supplementary Material showing further details on specific interferograms, close-up on the fractures mapped and comparison figures with previous datasets.

Supplementary Information The online version contains supplementary material available at <https://doi.org/10.1007/s00445-023-01699-0>.

Acknowledgements TerraSAR-X data from German Aerospace Center (DLR) was obtained via the Icelandic Volcanoes Supersite initiative (<http://geo-gsnl.org/supersites/permanent-supersites/iceland-volcanoes-supersite/>) through the Committee on Earth and Observing Satellites (CEOS). We used *Scientific colour maps* for the data visualization of this article (Cramer et al. 2020; Cramer 2021). All the figures were generated using the GMT software (Wessel et al. 2019). This study benefited from discussions with Oliver D. Lamb (Te Pū Ao | GNS Science), Sigríður Kristjánsdóttir (Icelandic Meteorological Office) and scientists of the University of Iceland. Comments from three anonymous reviewers and the Editor Prof. A. Tibaldi helped us improve the manuscript.

Author contribution CD, TA, PE, SJ, VD and HG designed the study. Generation of the interferograms was performed by CD with help from VD. Data analysis was carried out by CD with helpful comments from co-authors. HG performed the normal stress modelling (Figure S20), with discussion from SJ, TA and CD. PE, SJ and TA provided key discussion points and significant improvements to the first draft by CD. All authors participated in discussion and read, commented on and approved the final manuscript.

Funding This research was funded via a NordVulk fellowship (2020), the Icelandic Research Fund (Rannís) grants 174377-052 and 228933-051, and University of Iceland Research fund (2021).

Availability of data and materials The mapped fractures dataset can be found here: <https://doi.org/10.5281/zenodo.10433761>. The seismic data belongs the Icelandic Meteorological Office, and is available at <https://skjalftalisa.vedur.is/#/page/map> (last accessed August 2022).

Declarations

Conflict of interest The authors declare no competing interests.

Open Access This article is licensed under a Creative Commons Attribution 4.0 International License, which permits use, sharing, adaptation, distribution and reproduction in any medium or format, as long as you give appropriate credit to the original author(s) and the source, provide a link to the Creative Commons licence, and indicate if changes were made. The images or other third party material in this article are included in the article's Creative Commons licence, unless indicated otherwise in a credit line to the material. If material is not included in the article's Creative Commons licence and your intended use is not permitted by statutory regulation or exceeds the permitted use, you will need to obtain permission directly from the copyright holder. To view a copy of this licence, visit <http://creativecommons.org/licenses/by/4.0/>.

References

- Árnadóttir T, Geirsson H, Einarsson P (2004) Coseismic stress changes and crustal deformation on the Reykjanes Peninsula due to triggered earthquakes on 17 June 2000. *J Geophys Res Solid Earth* 109(B9). <https://doi.org/10.1029/2004JB003130>
- Árnadóttir T, Lund B, Jiang W et al (2009) Glacial rebound and plate spreading: Results from the first countrywide GPS observations in Iceland. *Geophys J Int* 177(2):691–716. <https://doi.org/10.1111/j.1365-246X.2008.04059.x>
- Barsotti S, Parks MM, Pfeffer MA et al (2023) The eruption in Fagradalsfjall (2021, Iceland): how the operational monitoring and the volcanic hazard assessment contributed to its safe access. *Nat Hazards*. <https://doi.org/10.1007/s11069-022-05798-7>
- Björnsson S, Einarsson P, Tulinius H et al (2020) Seismicity of the Reykjanes Peninsula 1971–1976. *J Volcanol Geotherm Res* 391(106):369. <https://doi.org/10.1016/j.jvolgeores.2018.04.026>
- Bufféral S, Panza E, Mannini S et al (2023) Surface fractures generated during the 2021 Reykjanes oblique rifting event (SW Iceland). *Bull Volcanol* 85(11):64. <https://doi.org/10.1007/s00445-023-01666-9>
- Chen CW, Zebker HA (2001) Two-dimensional phase unwrapping with use of statistical models for cost functions in nonlinear optimization. *JOSA A* 18(2):338–351. <https://doi.org/10.1364/JOSAA.18.000338>
- Clifton AE, Kattenhorn SA (2006) Structural architecture of a highly oblique divergent plate boundary segment. *Tectonophysics* 419(1):27–40. <https://doi.org/10.1016/j.tecto.2006.03.016>
- Clifton AE, Schlische RW (2003) Fracture populations on the Reykjanes Peninsula, Iceland: Comparison with experimental clay models of oblique rifting. *J Geophys Res Solid Earth* 108(B2). <https://doi.org/10.1029/2001JB000635>
- Cramer F (2021). *Scientific colour maps*. <https://doi.org/10.5281/zenodo.5501399>
- Cramer F, Shephard GE, Heron PJ (2020) The misuse of colour in science communication. *Nat Commun* 11(11):5444. <https://doi.org/10.1038/s41467-020-19160-7>
- Cubuk-Sabuncu Y, Jónsdóttir K, Caudron C et al (2021) Temporal Seismic Velocity Changes During the 2020 Rapid Inflation at Mt. Thorbjörn-Svartsengi, Iceland, Using Seismic Ambient Noise. *Geophys Res Lett* 48(11). <https://doi.org/10.1029/2020GL092265>
- Dobre C, Peltzer G (2007) Fluid-controlled faulting process in the Asal Rift, Djibouti, from 8 yr of radar interferometry observations. *Geology* 35(1):69–72. <https://doi.org/10.1130/G23022A.1>
- Ducrocq C, Geirsson H, Árnadóttir T et al (2021) Inflation-Deflation Episodes in the Hengill and Hrómundartindur Volcanic Complexes. SW Iceland. *Front Earth Sci* 9:915. <https://doi.org/10.3389/feart.2021.725109>
- Dumont S, Socquet A, Grandin R et al (2016) Surface displacements on faults triggered by slow magma transfers between dyke injections in the 2005–2010 rifting episode at Dabbahu-Manda-Hararo rift (Afar, Ethiopia). *Geophys J Int* 204(1):399–417. <https://doi.org/10.1093/gji/ggv449>
- Eibl EPS, Thordarson T, Höskuldsson A et al (2023) Evolving shallow conduit revealed by tremor and vent activity observations during episodic lava fountaining of the 2021 Geldingadalir eruption. Iceland. *Bull Volcanol* 85(2):10. <https://doi.org/10.1007/s00445-022-01622-z>
- Einarsson P (2008) Plate boundaries, rifts and transforms in Iceland. *Jökull* 58(58):35–58
- Einarsson P, Brandsdóttir B (2021) Seismicity of the Northern Volcanic Zone of Iceland. *Frontiers in Earth Science* 9. <https://www.frontiersin.org/articles/10.3389/feart.2021.628967>
- Einarsson P, Hjartardóttir AR, Hreinsdóttir S et al (2020) The structure of seismogenic strike-slip faults in the eastern part of the Reykjanes Peninsula Oblique Rift, SW Iceland. *J Volcanol Geotherm Res* 391(106):372. <https://doi.org/10.1016/j.jvolgeores.2018.04.029>
- Einarsson P, Eyjólfsson V, Hjartardóttir AR (2023) Tectonic framework and fault structures in the Fagradalsfjall segment of the Reykjanes Peninsula Oblique Rift, Iceland. *Bull Volcanol* 85(2):9. <https://doi.org/10.1007/s00445-022-01624-x>
- Feigl KL, Gasperi J, Sigmundsson F et al (2000) Crustal deformation near Hengill volcano, Iceland 1993–1998: Coupling between magmatic activity and faulting inferred from elastic modeling of satellite radar interferograms. *J Geophys Res Solid Earth* 105(B11):25,655–25,670. <https://doi.org/10.1029/2000JB900209>
- Fischer T, Hrubcová P, Salama A et al (2022) Swarm seismicity illuminates stress transfer prior to the 2021 Fagradalsfjall eruption

- in Iceland. *Earth Planet Sci Lett* 594(117):685. <https://doi.org/10.1016/j.epsl.2022.117685>
- Flóvenz OG, Wang R, Hersir GP, et al. (2022) Cyclical geothermal unrest as a precursor to Iceland's 2021 Fagradalsfjall eruption. *Nature Geoscience* pp 1–8. <https://doi.org/10.1038/s41561-022-00930-5>
- Geirsson H, Parks M, Vogfjörð K, et al. (2021) The 2020 volcano-tectonic unrest at Reykjanes Peninsula, Iceland: stress triggering and reactivation of several volcanic systems pp EGU21–7534. <https://doi.org/10.5194/egusphere-egu21-7534>
- Goldstein RM, Werner CL (1998) Radar interferogram filtering for geophysical applications. *Geophys Res Lett* 25(21):4035–4038. <https://doi.org/10.1029/1998GL900033>
- Gudjónsdóttir SR, Ilyinskaya E, Hreinsdóttir S et al (2020) Gas emissions and crustal deformation from the Krýsuvík high temperature geothermal system, Iceland. *J Volcanol Geotherm Res* 391(106):350. <https://doi.org/10.1016/j.jvolgeores.2018.04.007>
- Heap MJ, Villeneuve M, Albino F et al (2020) Towards more realistic values of elastic moduli for volcano modelling. *J Volcanol Geotherm Res* 390(106):684. <https://doi.org/10.1016/j.jvolgeores.2019.106684>
- Hjartardóttir AR, Einarsson P, Bramham E et al (2012) The Krafla fissure swarm, Iceland, and its formation by rifting events. *Bull Volcanol* 74(9):2139–2153. <https://doi.org/10.1007/s00445-012-0659-0>
- Hjartardóttir AR, Einarsson P, Gudmundsson MT et al (2016) Fracture movements and graben subsidence during the 2014 Bárðarbunga dike intrusion in Iceland. *J Volcanol Geotherm Res* 310:242–252. <https://doi.org/10.1016/j.jvolgeores.2015.12.002>
- Hjartardóttir AR, Dürig T, Parks M et al (2023) Pre-existing fractures and eruptive vent openings during the 2021 Fagradalsfjall eruption. *Iceland. Bull Volcanol* 85(10):56. <https://doi.org/10.1007/s00445-023-01670-z>
- Hreinsdóttir S, Einarsson P, Sigmundsson F (2001) Crustal deformation at the oblique spreading Reykjanes Peninsula, SW Iceland: GPS measurements from 1993 to 1998. *J Geophys Res Solid Earth* 106(B7):13,803–13,816. <https://doi.org/10.1029/2001JB000428>
- Hrubcová P, Vavryčuk V (2023) Tectonic stress changes related to plate spreading prior to the 2021 Fagradalsfjall eruption in SW Iceland. *Tectonophysics* 851(229):761. <https://doi.org/10.1016/j.tecto.2023.229761>
- Jónasson K, Besson B, Helgadóttir A et al (2021) A harmonised instrumental earthquake catalogue for Iceland and the northern Mid-Atlantic Ridge. *Nat Hazards Earth Syst Sci* 21(7):2197–2214. <https://doi.org/10.5194/nhess-21-2197-2021>
- Jónsson S (2009) Anthropogenic and Natural Deformation on Reykjanes Peninsula, Southwest Iceland, observed using InSAR Time-Series Analysis 1992–2008. EGU General Assembly, 5142
- Kampes BM, Hanssen RF, Perski Z (2003) Radar Interferometry with Public Domain Tools. Proceedings of FRINGE 2003, December 1–5, Frascati, Italy
- Keiding M, Árnadóttir T, Sturkell E et al (2008) Strain accumulation along an oblique plate boundary: The Reykjanes Peninsula, southwest Iceland. *Geophys J Int* 172(2):861–872. <https://doi.org/10.1111/j.1365-246X.2007.03655.x>
- Keiding M, Lund B, Árnadóttir T (2009) Earthquakes, stress, and strain along an obliquely divergent plate boundary: Reykjanes Peninsula, southwest Iceland. *J Geophys Res Solid Earth* 114(B9). <https://doi.org/10.1029/2008JB006253>
- Keiding M, Árnadóttir T, Jónsson S et al (2010) Plate boundary deformation and man-made subsidence around geothermal fields on the Reykjanes Peninsula, Iceland. *J Volcanol Geotherm Res* 194(4):139–149. <https://doi.org/10.1016/j.jvolgeores.2010.04.011>
- Kühn D, Dahm T (2008) Numerical modelling of dyke interaction and its influence on oceanic crust formation. *Tectonophysics* 447(1–4):53–65. <https://doi.org/10.1016/j.tecto.2006.09.018>
- Lamb OD, Gestrich JE, Barne TD et al (2022) Acoustic observations of lava fountain activity during the 2021 Fagradalsfjall eruption. *Iceland. Bull Volcanol* 84(11):96. <https://doi.org/10.1007/s00445-022-01602-3>
- Michalczyńska K, Hreinsdóttir S, Arnadóttir T, et al. (2012) Inflation and deflation episodes in the Krisuvik volcanic system. vol 2012. AGU, pp V33A–2843, aDS Bibcode: 2012AGUFM.V33A2843M
- Monaco C, Catalano S, Cocina O et al (2005) Tectonic control on the eruptive dynamics at Mt. Etna Volcano (Sicily) during the 2001 and 2002–2003 eruptions. *J Volcanol Geotherm Res* 144(1):211–233. <https://doi.org/10.1016/j.jvolgeores.2004.11.024>
- Pagli C, Pedersen R, Sigmundsson F et al (2003) Triggered fault slip on June 17, 2000 on the Reykjanes Peninsula, SW-Iceland captured by radar interferometry. *Geophys Res Lett* 30(6). <https://doi.org/10.1029/2002GL015310>
- Panzer F, Zechar JD, Vogfjörð KS et al (2016) A Revised Earthquake Catalogue for South Iceland. *Pure Appl Geophys* 173(1):97–116. <https://doi.org/10.1007/s00024-015-1115-9>
- Pedersen GBM, Belart JMC, Óskarsson BV et al (2022) Volume, Effusion Rate, and Lava Transport During the 2021 Fagradalsfjall Eruption: Results From Near Real-Time Photogrammetric Monitoring. *Geophys Res Lett* 49(13):e2021GL097125. <https://doi.org/10.1029/2021GL097125>
- Porter C, Morin P, Howat I et al (2018) ArcticDEM, Version 3. Harvard Dataverse V1. <https://doi.org/10.7910/DVN/OHHUKH>
- QGIS Development Team (2021) QGIS Geographic Information System. QGIS Association, <http://qgis.org>
- Richter N, Poland MP, Lundgren PR (2013) TerraSAR-X interferometry reveals small-scale deformation associated with the summit eruption of Kilauea Volcano, Hawai'i. *Geophys Res Lett* 40(7):1279–1283. <https://doi.org/10.1002/grl.50286>
- Ruch J, Wang T, Xu W et al (2016) Oblique rift opening revealed by reoccurring magma injection in central Iceland. *Nat Commun* 7(11):12,352. <https://doi.org/10.1038/ncomms12352>
- Sæmundsson K, Sigurgeirsson MA, Fridleifsson GO (2020) Geology and structure of the Reykjanes volcanic system, Iceland. *J Volcanol Geotherm Res* 391(106):501. <https://doi.org/10.1016/j.jvolgeores.2018.11.022>
- Seebeck H, Nicol A (2009) Dike intrusion and displacement accumulation at the intersection of the Okataina Volcanic Centre and Paeroa Fault zone. Taupo Rift, New Zealand. *Tectonophysics* 475(3):575–585. <https://doi.org/10.1016/j.tecto.2009.07.009>
- Sigmundsson F, Parks M, Hooper A, et al. (2022) Deformation and seismicity decline before the 2021 Fagradalsfjall eruption. *Nature* pp 1–6. <https://doi.org/10.1038/s41586-022-05083-4>
- Spacapan JB, Galland O, Leanza HA et al (2016) Control of strike-slip fault on dyke emplacement and morphology. *J Geol Soc* 173(4):573–576. <https://doi.org/10.1144/jgs2015-166>
- Sudhaus H, Jónsson S (2009) Improved source modelling through combined use of InSAR and GPS under consideration of correlated data errors: application to the June 2000 Kleifarvatn earthquake. *Iceland. Geophys J Int* 176(2):389–404. <https://doi.org/10.1111/j.1365-246X.2008.03989.x>
- Venzke E (2023) Global Volcanism Program 2023. [Database] Volcanoes of the World, version 5.1.0. Distributed by Smithsonian Institution, compiled by Venzke, E <https://doi.org/10.5479/si.GVP.VOTW5-2023.5.1>
- Villamor P, Berryman K, Nairn I et al (2011) Associations between volcanic eruptions from Okataina volcanic center and surface rupture of nearby active faults, Taupo rift, New Zealand: Insights into

- the nature of volcano-tectonic interactions. *GSA Bulletin* 123(7–8):1383–1405. <https://doi.org/10.1130/B30184.1>
- Villamor P, Litchfield NJ, Gómez-Ortiz D et al (2022) Fault ruptures triggered by large rhyolitic eruptions at the boundary between tectonic and magmatic rift segments: The Manawahe Fault, Taupo Rift, New Zealand. *J Volcanol Geotherm Res* 427(107):478. <https://doi.org/10.1016/j.jvolgeores.2022.107478>
- Wessel P, Luis JF, Uieda L et al (2019) The Generic Mapping Tools Version 6. *Geochem Geophys Geosystems* 20(11):5556–5564. <https://doi.org/10.1029/2019GC008515>

Publisher's Note Springer Nature remains neutral with regard to jurisdictional claims in published maps and institutional affiliations.